



Letter

Development of nano-alumina based ceramic components for high heat flux insulation applications under dynamic load

Sarika Mishra*, Rati Ranjana, K. Balasubramanian

Non-Ferrous Materials Technology Development Centre, P.O. Kanchanbagh, Hyderabad 500058, India

ARTICLE INFO

Article history:

Received 20 December 2011
 Received in revised form 25 January 2012
 Accepted 27 January 2012
 Available online 7 February 2012

Keywords:

Nano-alumina ceramics
 Insulators
 Combustion synthesis
 X-ray diffraction
 Microstructure
 Thermal shock resistance

ABSTRACT

Attempts have been made towards the synthesis of nano-alumina powder through conventional combustion synthesis (CCS) method. Detailed evaluation of the process parameters has been done through XRD and SEM, on the as-synthesized nano-alumina powders. The as-synthesized nano-alumina (γ phase) were used for developing ceramic spacers for thermal insulation application under load. The densification and mechanical strength of ceramic components consolidated from the alumina powders has been measured. The results have shown that the as-fabricated nano-alumina based components have high structural integrity at green stage ($\sim 65\%$) with 2 wt.% nano γ -alumina, significant mechanical strength (~ 230 MPa) and excellent thermal shock resistance (functional testing at $\sim 1400^\circ\text{C}$ temperature and under 50 T dynamic load). The comprehensive study for the fabrication of nano-alumina based ceramic spacers has been illustrated.

© 2012 Elsevier B.V. All rights reserved.

1. Introduction

High density ceramic components with controlled and uniform microstructures required for advanced engineering applications necessitates powders with narrow particle size distribution, fineness and desired morphology. Nano-crystalline alumina (Al_2O_3) has considerable potential for various applications for its usage as coating material [1], thermal insulation [2], pollution prevention [3], sintering aid for ceramic [4], and biocompatible material for medical and dental composites [5,6]. Various preparatory methods such as co-precipitation [7,8], sol-gel [9,10] and combustion synthesis [11–13,2,14] have been developed for the preparation of nano-crystalline Al_2O_3 powders. Among these methods, the combustion synthesis process is the most common method of producing nano-alumina as it is easy and less energy-intensive [7,15,16]. Moreover, the solution based combustion synthesis is advantageous over the solid-state synthesis in terms of better compositional homogeneity and purity of the final product [17,18].

The combustion synthesis reaction is usually carried out with different heating mediums (conventional resistance and microwave F/c). The basis of the combustion synthesis technique comes from the thermo-chemical concepts used in the field of propellants and explosives. The parameters that influence the reaction in combustion synthesis are type of fuel, fuel to oxidizer ratio, use

of excess oxidizer, ignition temperature and water content of the mixture [12]. The α - and γ -alumina are the only two types of nano-alumina that are produced. The crystal structure of α -alumina is a hexagonal plate with large surface area. This geometry enables alumina for its usage in catalytic and adsorbent applications.

In this paper, the synthesis of α -alumina and γ -alumina powders using conventional combustion synthesis (CCS) is reported. The effect of different fuel-to-oxidant ratios, sintering temperatures, and type of fuel on phases formed in the synthesized powder has been studied. The development of ceramic components from these as synthesized alumina powders and their enhanced properties due to nano-powder addition has also been illustrated.

2. Experimental procedure

2.1. Raw materials

Chemical grade aluminium nitrate [$\text{Al}(\text{NO}_3)_3 \cdot 9\text{H}_2\text{O}$], dextrose ($\text{C}_6\text{H}_{12}\text{O}_6$), urea (NH_2CONH_2), and glycine ($\text{NH}_2\text{CH}_2\text{CO}_2\text{H}$) (all from Finar reagents, extrapure) were used as precursor materials for this study.

2.2. Powder synthesis

2.2.1. Conventional combustion synthesis (CCS)

Combustion synthesis was carried out on mixtures of aluminium nitrate (oxidant) with different fuels such as urea, glycine, and dextrose. Different oxidant-to-fuel ratios in the range of 1.2–3.5 were employed for synthesizing nano-alumina. The reagent solutions were mixed simultaneously and heated at 150°C for gelation. The as-synthesized gels were calcined at ~ 300 – 900°C temperature for obtaining nano α -alumina and γ -alumina. The phase analysis, and microstructure in the resulting alumina powders was examined by XRD (Philips, Panalytical) and SEM

* Corresponding author. Tel.: +91 040 24341332; fax: +91 040 24342567.
 E-mail address: uptecsarika@rediffmail.com (S. Mishra).

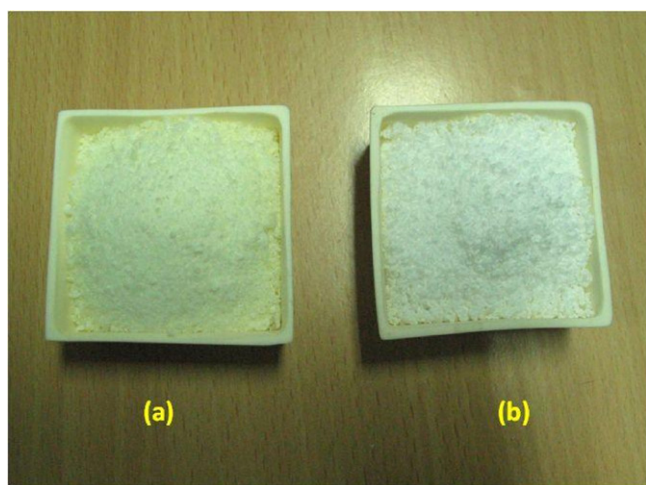


Fig. 1. CCS synthesized nano-alumina powders; (a) gamma alumina, and (b) alpha alumina.

(VEGA TESCAN), respectively. The crystallite sizes on the as-synthesized nano-alumina powders were calculated using the Scherrer formula.

2.3. Fabrication of ceramic component

The as-synthesized nano-alumina powders were used for the fabrication of ceramic spacers through powder metallurgy route for high temperature thermal insulation application under load conditions. These insulators were formed with commercial alumina powder ($d_{50} = 1.5 \mu\text{m}$), and as-synthesized nano-alumina powder (1–5 wt.%) blended commercial alumina. The pellets (33.3 mm dia., 10.54 mm height) were first axially pressed compacted at 200–280 MPa and then pre-sintered at 1000 °C to enable strength for the green machining to near-net shape. The pre-sintered pellets were carefully machined using CNC machining to the functional dimensions. Subsequently, the machined components were sintered at 1600 °C for 1 h in air atmosphere. The densities of the as sintered components were measured by Archimedes method. The strength of the as-fabricated ceramic component was measured through 3-point bend test.

3. Results and discussions

3.1. Nano-alumina powder

The nano-alumina powders prepared through CCS method are shown in Fig. 1. The color difference is visible for alpha ($-\alpha$) [pure white] and gamma ($-\gamma$) alumina [off-white] powders. Fig. 2 shows

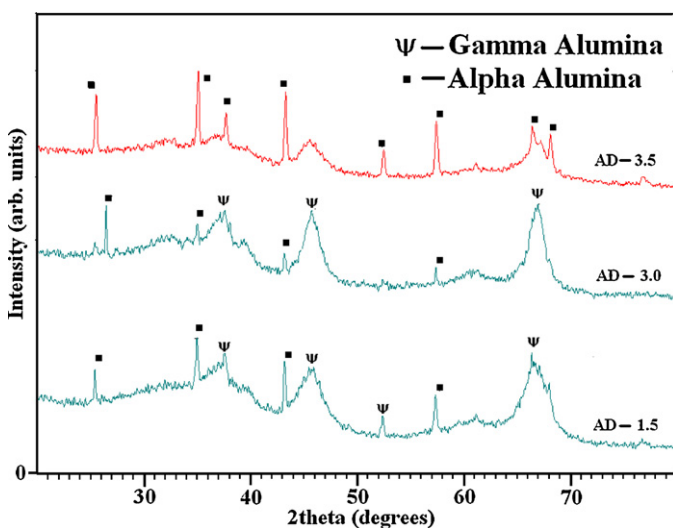


Fig. 2. XRD patterns of nano-alumina made with dextrose as fuel at different ratios.

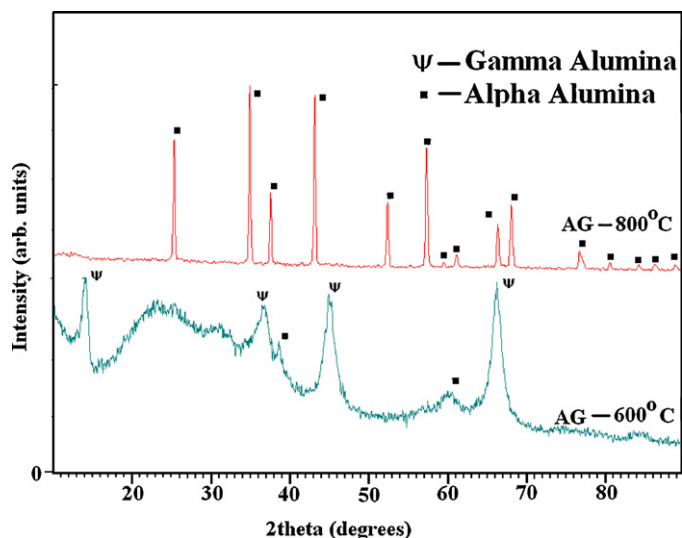


Fig. 3. XRD patterns of nano-alumina (glycine as fuel) calcined at different temperatures (Ψ – gamma alumina; ■ – alpha alumina).

the XRD patterns of nano-alumina obtained with dextrose (AD) as the fuel in different oxidant-to-fuel ratios (1.5–3.5). It is evident from Fig. 2 that the content of alpha ($-\alpha$) and gamma ($-\gamma$) phase in the nano-alumina powder varies with the oxidant-to-fuel ratio. With the increasing oxidant-to-fuel ratios, the alpha phase predominates.

Fig. 3 indicates the effect of calcinations temperature on the phases formed in the nano-alumina obtained with glycine (AG) as the fuel. An amorphous mixture of ($-\gamma$) and ($-\alpha$) phase in the nano-alumina powder is obtained with a partial crystallinity at combustion temperature of 600 °C whereas at 800 °C a fully crystalline ($-\alpha$) phase predominates (Fig. 3). Wherein with glycine as fuel, the process has resulted into some ($-\gamma$) phase peaks at 600 °C (Fig. 3), with the use of urea as fuel (AU), the presence of ($-\gamma$) alumina phase is observed up to 300 °C only (Fig. 4). Moreover, the amorphous form of nano-alumina (with urea as fuel) is present up to 300 °C and beyond that it becomes crystalline. The nature of combustion and variation in the powder characteristics obtained from different fuel-to-oxidant ratios can be explained on the basis of phase formation at different stoichiometric ratios and variation

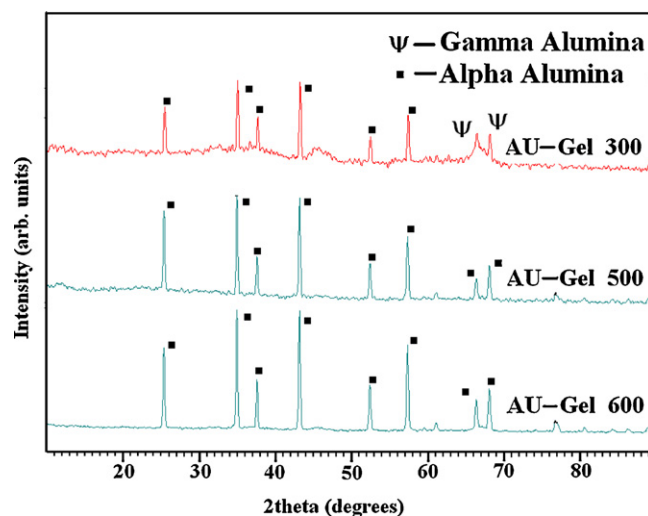


Fig. 4. XRD patterns of nano-alumina (urea as fuel) calcined at different temperatures (Ψ – gamma alumina; ■ – alpha alumina).

Table 1
Crystallite sizes of nano-alumina powders prepared using various fuels.

Fuel	Phase	Crystallite size, nm (with calcination temp.)	Crystallite size, nm (with fuel ratio)
Urea	γ -Alumina	880	81
	α -Alumina	99	19
Glycine	γ -Alumina	65	17
	α -Alumina	17	12
Dextrose	γ -Alumina	48	86
	α -Alumina	97	9

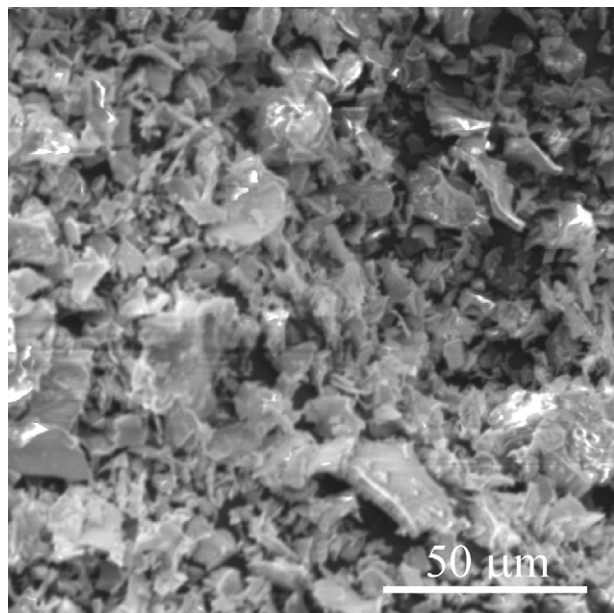


Fig. 5. SEM micrograph of as-synthesized nano-alumina powder.

of temperatures since the nature of agglomeration (hard or soft) is governed from temperature generated during combustion. The crystallite sizes obtained in nano-alumina powders estimated from the FWHM values of XRD peaks are shown in Table 1 for comparison purpose. The microstructure of as-synthesized nano-alumina powder shows an amorphous flaky structure with an average agglomerate size of ~ 5 – $10 \mu\text{m}$ (Fig. 5).



Fig. 6. Digital picture of as fabricated nano-alumina based ceramic spacers.

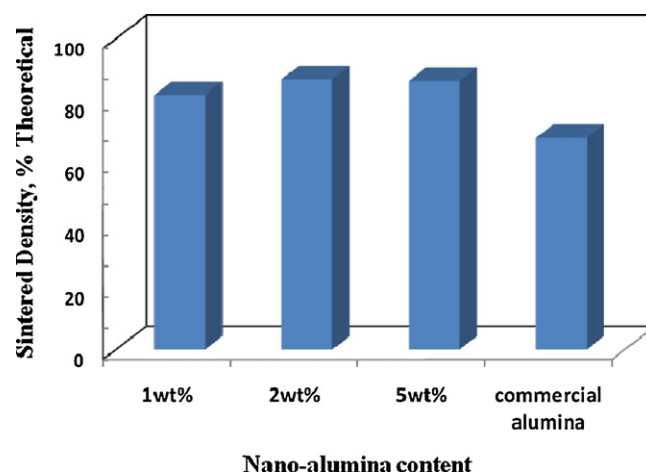


Fig. 7. Plot showing the effect of extent of nano-alumina addition on the sintered density of the ceramic component.

3.2. Nano-alumina based component

The as-fabricated nano-alumina based components (Fig. 6) have shown a significant improvement in the sintered density with the incorporation of nano-alumina in the commercial alumina powder (Fig. 7). It can also be seen from Fig. 7 that a density as high as 96% could be achieved at a relatively low sintering temperature of 1600°C , with the blending of 2 wt.% γ -alumina with commercial alumina (average green density $\sim 64\%$). The 3-point bend strength of the nano-alumina based ceramic components was recorded as high as $\sim 230 \text{ MPa}$. These components have been successfully tested for the functional test (through copper melting) under dynamic load (50 T) and high temperature thermal shock (~ 1400 – 1450°C) conditions.

4. Conclusion

Nano-alumina powders have been synthesized through a cost effective combustion synthesis route. The process has been optimized in terms of fuel type, oxidant-to-fuel ratio and combustion temperatures. The extent of conversion from γ to α -alumina phase has been shown to depend on the temperature and time of calcinations. The as-synthesized nano-alumina powder has been used to successfully fabricate ceramic insulators (spacers) for high temperature thermal insulation application under load conditions. The 3-point bend strength of the nano-alumina based ceramic components was recorded as high as $\sim 230 \text{ MPa}$. The as-fabricated components were found to be excellent in terms of sintered density ($\sim 96\%$), mechanical strength and high temperature thermal shock resistance (functionally validated at $\sim 1400^\circ\text{C}$ temperature and under 50 T dynamic load). The addition of nano-alumina enhances the product functional performance and hence the process owes the potential for fabricating larger ceramic components.

Acknowledgement

The authors are grateful to Mr. D. Lokeswara Rao, Deputy Project Director, NFTDC for providing support towards carrying out this work.

References

- [1] J. He, J.M. Schoenung, Mater. Sci. Eng. A 336 (2002) 274–319.
- [2] J.C. Toniolo, M.D. Lima, A.S. Takimi, C.P. Bergmann, Mater. Res. Bull. 40 (2005) 561–571.
- [3] A. Khaleel, P.N. Kapoor, K.J. Klabunde, Nanostruct. Mater. 11 (1999) 459–468.

- [4] R.J. Hellmig, J.F. Castagnet, H. Ferkel, *Nanostruct. Mater.* 12 (1999) 1041–1044.
- [5] R.W. Siegel, T.J. Webster, *Nanostruct. Mater.* 12 (1999) 983–986.
- [6] L.G. Gutwein, T.J. Webster, *Biomaterials* 25 (2004) 4175–4183.
- [7] T.Y. Peng, P.W. Du, B. Hu, Z.C. Jiang, *J. Inorg. Mater.* 15 (2000) 1097–1101.
- [8] S. Ramanathan, S.K. Roy, R. Bhat, D.D. Upadhaya, A.R. Biswas, *J. Alloys Compd.* 243 (1996) 39–44.
- [9] S. Kureti, W. Weisweiler, *J. Non-Cryst. Solids* 303 (2002) 253–261.
- [10] F. Mirjalili, M. Hasmaliza, L.C. Abdullah, *Ceram. Int.* 36 (2010) 1253–1257.
- [11] T. Peng, X. Liu, K. Dai, J. Xiao, H. Song, *Mater. Res. Bull.* 41 (2006) 1638–1645.
- [12] K.C. Patil, S.T. Aruna, T. Mimani, *Curr. Opin. Solid State Mater. Sci.* 6 (2002) 507–512.
- [13] A.S. Mukasyan, P. Epstein, P. Dinka, *Proc. Combust. Inst.* 31 (2007) 1789–1795.
- [14] S.T. Aruna, A.S. Mukasyan, *Curr. Opin. Solid State Mater. Sci.* 12 (2008) 44–50.
- [15] H.C. Park, Y.J. Park, R. Stevens, *Mater. Sci. Eng. A* 367 (2004) 166–170.
- [16] M.S. Tsai, F.H. Yung, F.H. Yang, *Ceram. Int.* 33 (2007) 739–745.
- [17] Y. Wu, A. Bandyopadhyay, S. Bose, *Mater. Sci. Eng. A* 380 (2004) 349–355.
- [18] I. Ganesh, P.M.C. Torres, J.M.F. Ferreira, *Ceram. Int.* 35 (2009) 1173–1179.